

Synthesis of Acrylamide-Based Block-Copolymer Brushes Under Flow: Monitoring Real-Time Growth and Surface Restructuring Upon Drying

Joydeb Mandal, Andrea Arcifa, Nicholas D. Spencer*

Laboratory for Surface Science and Technology, Department of Materials, ETH Zurich,
Vladimir-Prelog-Weg 5, CH-8093 Zurich, Switzerland

SUPPLEMENTARY INFORMATION

A. Preparation of Reaction Mixtures

N,N-dimethylacrylamide (DMAM)

A mixture of 4 g (40.35 mmol) DMAM, 43 μ L (0.16 mmol) Me6TREN, 0.8 g (4.8 mmol) tEtAmCl, 5.4 mg CuCl₂ (0.04 mmol) and 10 mL 80:20 ethanol/water mixture was degassed by bubbling nitrogen gas for 45 minutes. The degassed solution was then transferred to a degassed flask containing 8 mg (0.08 mmol) of CuCl using a degassed syringe. The solution was then stirred for 10 minutes under N₂ atmosphere until complete dissolution of the catalyst.

N-Hydroxyethyl acrylamide (HEAM)

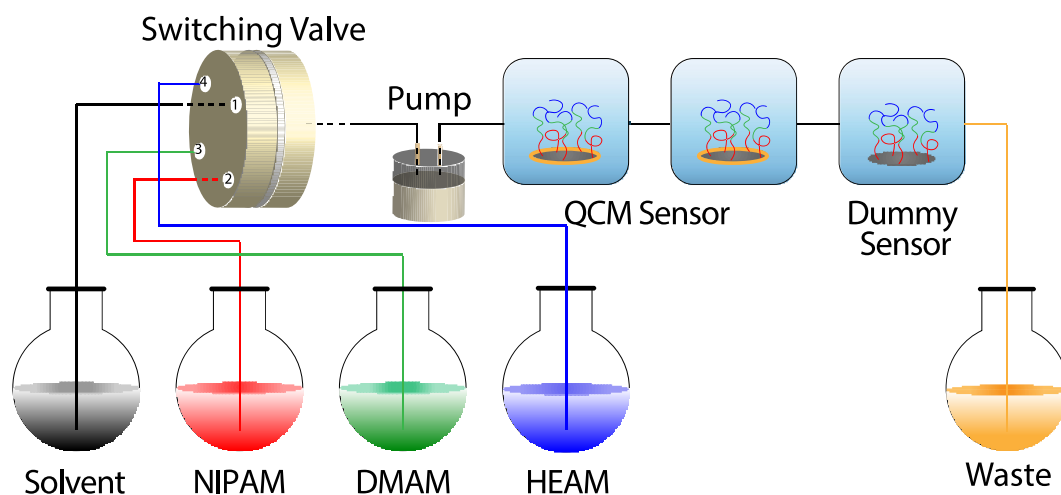
4.65 g (40.35) HEAM, 43 μ L (0.16 mmol) Me6TREN, 0.27 g (1.6 mmol) tEtAmCl and 2.2 mg CuCl₂ (0.016 mmol) were dissolved in 10 mL 80:20 ethanol/water mixture. The reaction mixture was then degassed by bubbling nitrogen gas for 45 minutes. The degassed solution was then transferred to a degassed flask containing 8 mg (0.08 mmol) of CuCl using a degassed syringe. The solution was then stirred for 10 minutes under N₂ atmosphere until complete dissolution of the catalyst.

N-Isopropylacrylamide (NIPAM)

4.57 g (40.35) HEAM, 43 μ L (0.16 mmol) Me6TREN, 0.84 g (4.0 mmol) tEtAmBr and 3.6 mg CuBr₂ (0.016 mmol) were dissolved in 10 mL 80:20 ethanol/water mixture. The reaction mixture was then degassed by bubbling nitrogen gas for 45 minutes. The degassed solution was then transferred to a degassed flask containing 11.6 mg (0.08 mmol) of CuBr using a degassed syringe. The solution was then stirred for 10 minutes under N₂ atmosphere until complete dissolution of the catalyst.

B. Flow Synthesis

At first, a baseline was achieved by flowing 80:20 ethanol/water (solvent) through the QCM-D cells. As soon as a stable baseline was established, the polymerization was initiated by switching the medium to one of the reaction mixtures using a multi-position selection valve (Vici, model no.: EUHA, Serial no.: EUA08048, Valco Instruments, Houston, Texas, USA) as shown in the Scheme 1. The reaction mixtures were switched from one to another depending on the desired sequence of the blocks of the block copolymer brushes. Finally, the medium was again switched back to 80:20 ethanol/water to cease the polymerization. The flow rate was maintained at $2.5 \mu\text{Ls}^{-1}$ using a piston pump (milliGAT Low Flow pump, Model CP-DSM-GF, Valco Instrument Co. Inc., Houston, Texas, USA).



Scheme S1. Schematic illustration of the flow setup used for the synthesis and *in situ* monitoring of the growth of the block copolymer brushes

C. Static Water Contact Angle of Homo- and Block-Copolymer Brushes

The growth of the block copolymer brushes was examined by measuring the static water contact angle after each block formation and comparing the values with that obtained from the corresponding homopolymer brush.

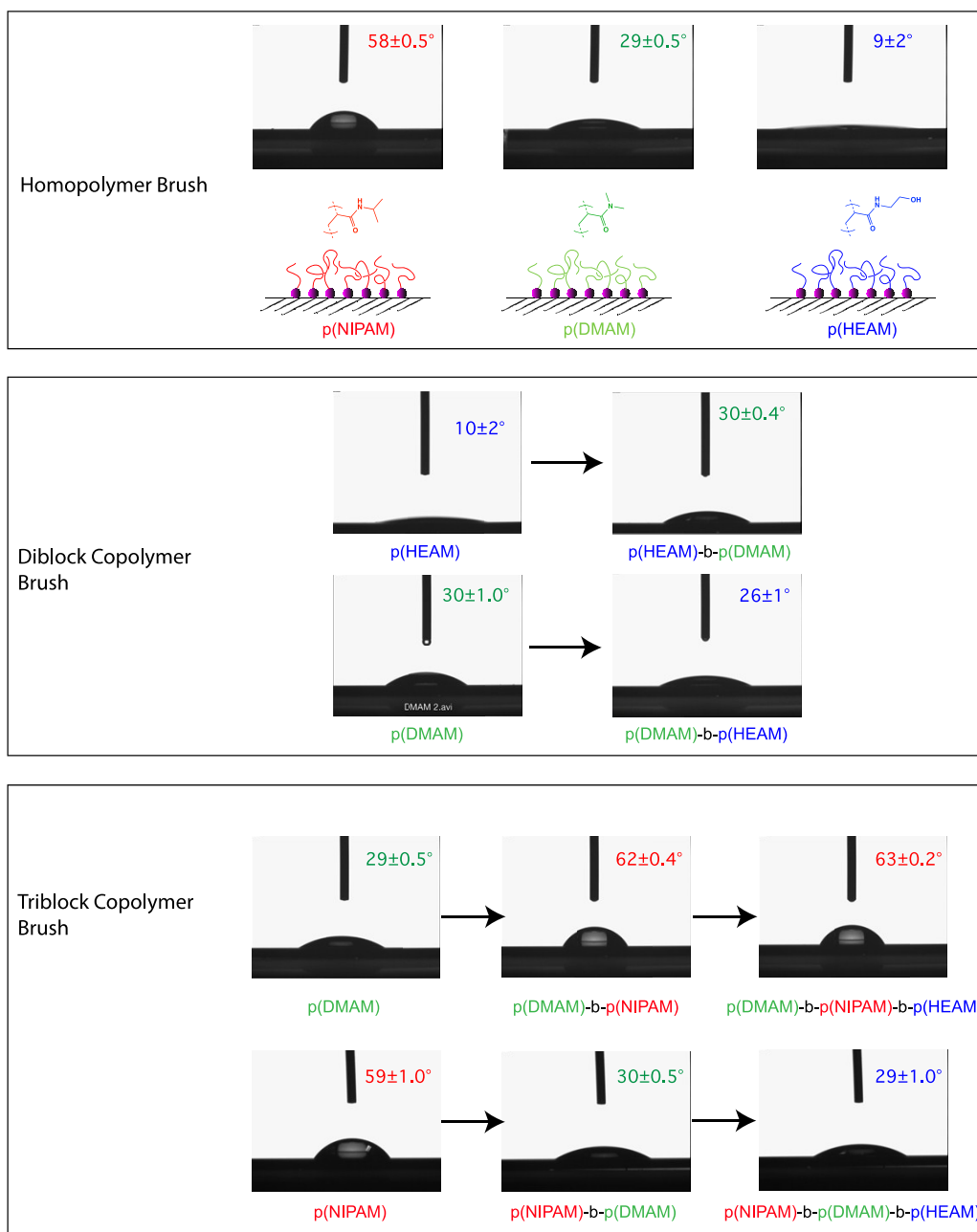


Figure S1. Static water contact angle (θ_w) of homo- and block-copolymer brushes. Each block was constructed by polymerizing the respective monomer for 20 min.

D. Dynamic Water Contact Angle of Homo and Block Copolymer Brushes

The advancing (θ_A) and receding (θ_R) contact angles of the homo- and block-copolymer brushes were measured with milli-Q water by addition to and withdrawal from a 5 μL drop at a rate of 4 $\mu\text{L min}^{-1}$. The contact hysteresis ($\Delta\theta = \theta_A - \theta_R$) observed for the block copolymer brushes was compared with that obtained from the homopolymer brush corresponding to the final block to understand the self-organization occurring in the block copolymer brushes.

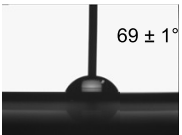
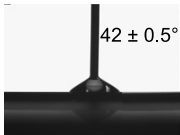
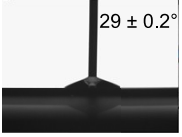
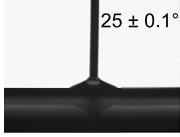

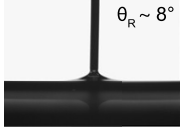
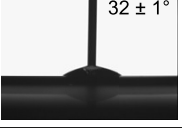
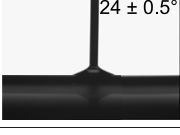
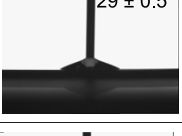
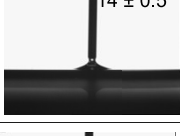
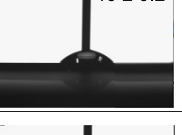
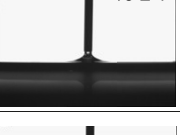
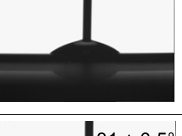
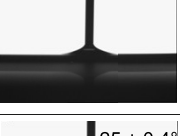

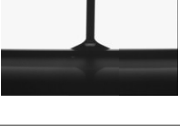
Sample	Advancing Contact Angle (θ_A)	Receding Contact Angle (θ_R)
p(NIPAM)	 69 ± 1°	 42 ± 0.5°
p(DMAM)	 29 ± 0.2°	 25 ± 0.1°
p(HEAM)	 $\theta_A \sim 8^\circ$	 $\theta_R \sim 8^\circ$
p(NIPAM)-b-p(DMAM)	 32 ± 1°	 24 ± 0.5°
p(NIPAM)-b-p(DMAM)-b-p(HEAM)	 29 ± 0.5°	 14 ± 0.5°
p(NIPAM)-b-p(HEAM)	 46 ± 0.2°	 13 ± 1°
p(DMAM)-b-p(HEAM)	 38 ± 0.5°	 13 ± 2°
p(HEAM)-b-p(DMAM)	 31 ± 0.5°	 25 ± 0.4°

Figure S2. Advancing (θ_A) and receding (θ_R) contact angles of homo- and block-copolymer brushes. Each block was constructed by polymerizing the respective monomer for 20 min.

E 1. Survey spectra: elemental analysis of the polymer brushes

The survey spectra of three homopolymers and three block copolymers discussed in this work are presented in Figure S3. The survey spectra reveal the presence of only elements (C, N, and O) that are expected to be present in the samples. Importantly, the lack of detectable signals corresponding to Si from the substrate (silicon wafers) indicates that the thicknesses of the dry polymer brushes were higher than the information depth (ID) of the technique.

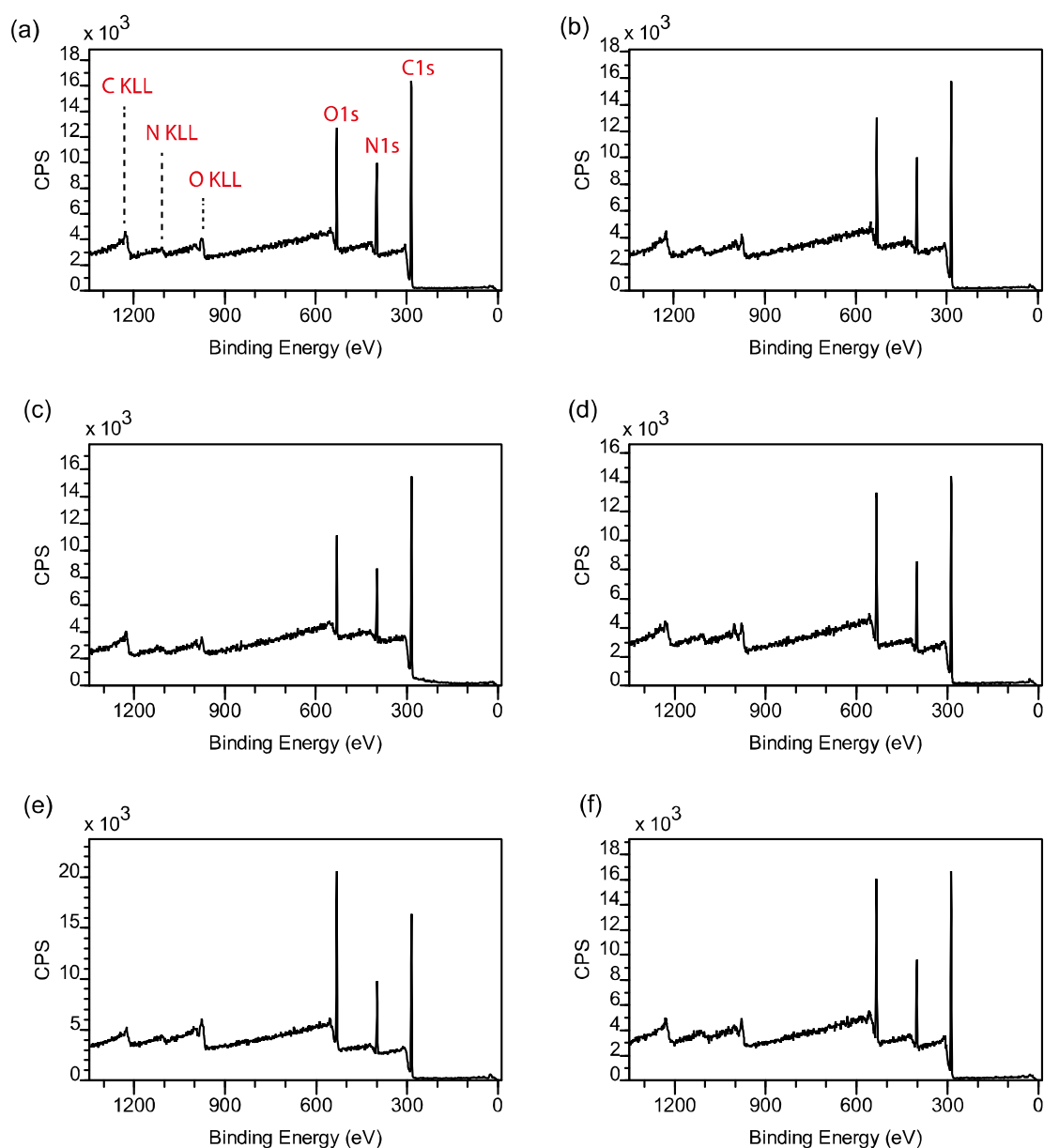


Figure S3: Survey XP-spectra of polymer brushes growth silicon wafers: (a) p(DMAM) (b) p(NIPAM)-b-p(DMAM), (c) p(NIPAM), (d) p(NIPAM)-b-p(DMAM)-b-p(HEAM) (e) p(HEAM), and (f) p(DMAM)-b-p(HEAM). The XP- and Auger signals of the detectable elements (carbon, nitrogen and oxygen) are labeled in (a).

E 2. High-resolution spectra: chemical-state analysis

HR spectra of three homopolymers presented in this work are shown in Figure S 4.

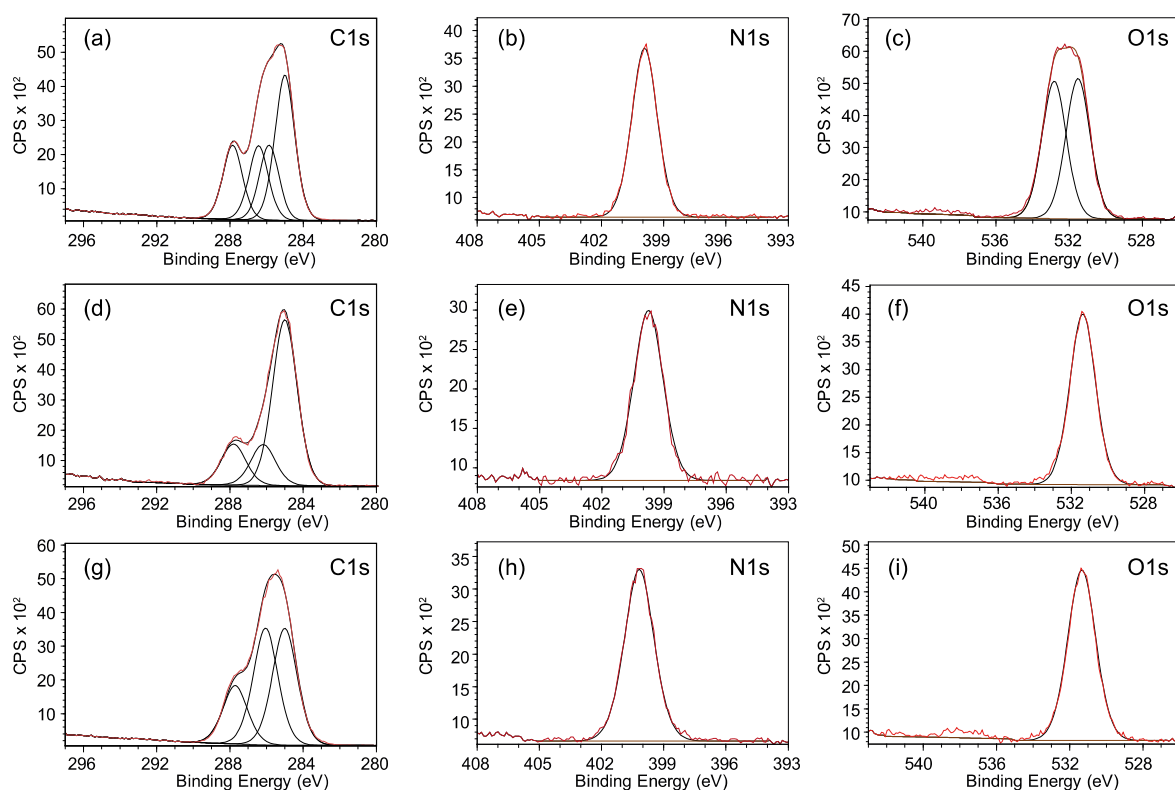


Figure S4. High-resolution XP-spectra of p(HEAM) (a-c), p(NIPAM) (d-f), and p(DMAM) (g-i). Raw data are reported in red. Black lines represent the fitting model (peaks, cumulative curve and background).

The signals in Figure S4 were fitted using the sums of Gaussian-Lorentzian product curves representing distinct chemical environments of an element. The following constraints were applied to fit the spectra:

- The relative intensities of the peaks used to fit the C1s HR-spectra reflect the expected stoichiometry of the materials.
- the full-width-at-half-maximum (FWHM) of all the C1s peaks was constrained to be the same for all the components.
- The O1s spectrum of p(HEAM) was fitted with two components representing the hydroxyl and carboxamide oxygen respectively. The constraints used for the C1s spectra were applied in this case as well (point a and b).

Table S1. The binding energies of the synthetic peaks representative of the various chemical states of carbon, oxygen and nitrogen obtained by using the curve-fitting model described above.

Signal	Chemical state	Binding energy (eV)		
		P(HEAM)	P(NIPAM)	P(DMAM)
C1s	C _{aliphatic}	285.0*	285.0*	285.0*
	C _{amide}	285.9	286.2	286.1
	C _{alcohol}	286.4	-	-
	C _{carboxamide}	287.9	287.8	287.7
O1s	O _{carboxamide}	531.5	531.4	531.3
	O _{hydroxyl}	532.8	-	-
N1s	N _{amide}	399.9	399.8	400.2

The values presented in the table are very similar to those reported by Beamson and Briggs^[1] for polymers carrying similar functional groups as in the polymer brushes presented in the present work.

Figure S 5a shows a comparison between the C1s spectrum of a p(NIPAM)-b-p(DMAM) brush and that of p(DMAM) brush. The two spectra clearly show a high degree of similarity. In contrast, the C1s spectrum of the block-copolymer clearly differs from that of the p(NIPAM) homopolymer brush (Figure S 5b).

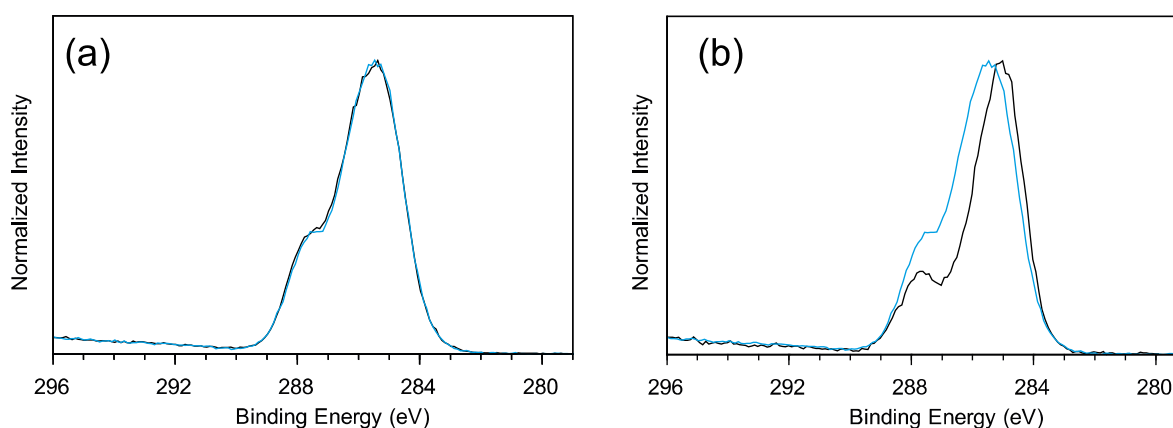


Figure S5. C1s spectrum of p(NIPAM)-b-p(DMAM) brush overlapped with that of p(DMAM) and p(NIPAM) brushes (a and b, respectively). A blue line is used for the spectrum of the block-copolymer; a black line is used for the spectra of the homopolymers.

Figure S6 shows the O1s spectrum of a p(NIPAM)-b-p(DMAM)-p(HEAM) copolymer brush. The above-discussed fitting model was applied, although in this case no constraint on the area of the two signals was applied. The ratio of the areas corresponding to carboxamide and hydroxyl components was found to be ~ 2.8 . Qualitatively, the results resemble those obtained for the p(DMAM)-p(HEAM) copolymer brush (Figure 4).

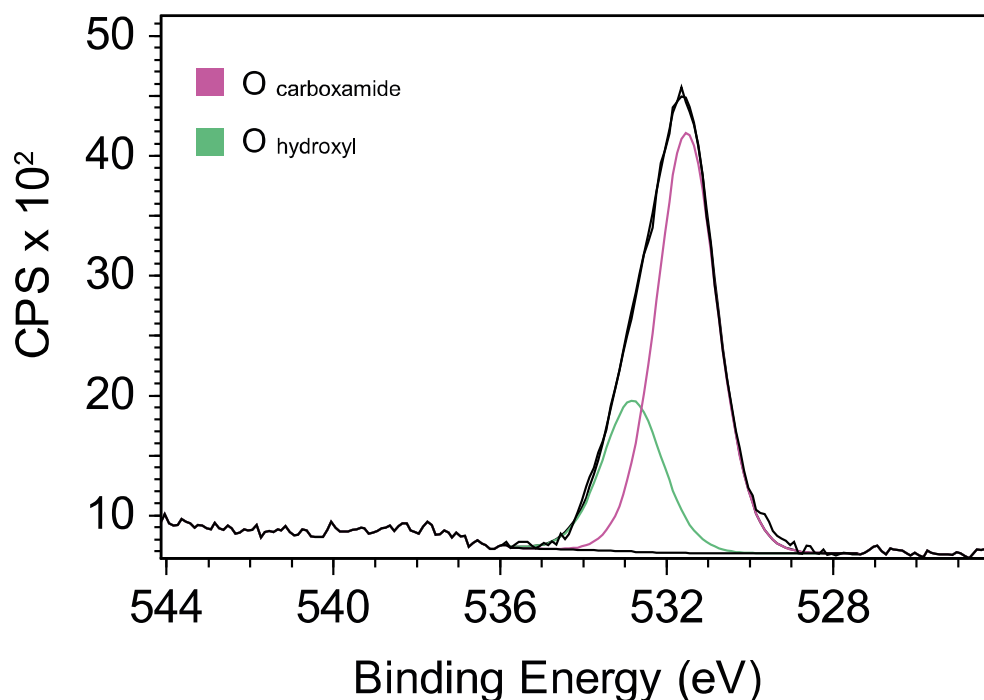


Figure S6. O1s spectrum of p(NIPAM)-b-p(DMAM)-p(HEAM) fitted with two components, representing the hydroxyl and the carboxamide oxygens.

E 3. Quantitative analysis

The atomic fraction of the detectable elements was estimated from the HR spectra, according to the following Equation S1 (ref):

$$\%x_a = \frac{RSF_a \cdot I_a}{\sum_i^n RSF_i \cdot I_i}$$

Eq. S1

S_i and I_i are the relative sensitivity factor (RSF) and the measured area of a XP-peak, respectively. RSFs were estimated using the *first-principles method*.^[2] This approach assumes that the material under investigation is homogeneous to a depth higher than the *information depth* (Section E 4).

Table S2 shows the results obtained with Eq S1, regardless of the chemical homogeneity near the surface (*apparent concentrations*).

Samples	C%	N%	O%
pNIPAM	76.4 (75.0)	11.8 (12.5)	11.8 (12.5)
pDMAM	72.8 (71.4)	13.8 (14.3)	13.4 (14.3)
pHEAM	64.7 (62.5)	11.8 (12.5)	23.5 (25.0)
pNIPAM-b-pDMAM	73.5	13.4	13.1
pDMAM-b-pHEAM	68.7	13.1	18.2
pNIPAM-pDMAM-b-pHEAM	69.7	13.6	16.7

*The values in brackets are the theoretical atomic concentrations of the polymers

** Hydrogen is not detectable by XPS, so it is not considered in quantitative analysis.

Table S2. Apparent concentrations of the individual elements (C, N, O) calculated to be present in the near-surface region of both homo- and block-copolymer brushes.

The apparent concentrations calculated for the homopolymers were found to be in good agreement with the expected stoichiometry of the materials. In line with the outcomes of the chemical-state analysis (Section E 2), this finding points to a compositional homogeneity of the homopolymer brushes within the information depth of the method.

E 4. Estimation of the information depth

The information depth (ID) is defined as the maximum normal depth from which information is obtained.

If the effect of elastic scattering can be neglected, the depth from which 99.7 % of the signals originates can be expressed as:

$$ID = 3 \cdot \lambda \cdot \cos \theta \quad \text{Equation S2}$$

where θ is the angle between the normal to the surface and the direction of the analyzer (emission angle), and λ is the inelastic mean free path (IMFP).

In this work, the Seah and Dench formula^[3] for organic materials was used to calculate the IMFP:

$$\lambda = 31 E^{-2} + 0.087 E^{0.5} \quad (\text{nm}) \quad \text{Equation S3}$$

where E is the kinetic energy of the photoelectron, in (eV).

Although, in general, the effects of elastic scattering on the attenuation of XP-signals cannot be neglected^[4], the formula is appropriate to describe the qualitative conclusions drawn in this study.

F4. Physical Adsorption of Monomer

To examine the effect of physical adsorption of monomers on the ΔF -t and ΔD -t profiles if there is any, we have carried out a controlled experiment in the absence of any ATRP-catalyst. The experiment was performed in the following way-

A QCM-D sensor, coated with ATRP-initiator was used to replicate the experimental condition as close as possible. A baseline was first achieved by flowing 80:20 ethanol/water (solvent) through the QCM-D cells. As soon as a stable baseline was established, the solvent was replaced by a solution of N-hydroxyethylacrylamide (HEAM) in 80:20 ethanol/water. Finally, the medium was again switched back to 80:20 ethanol/water.

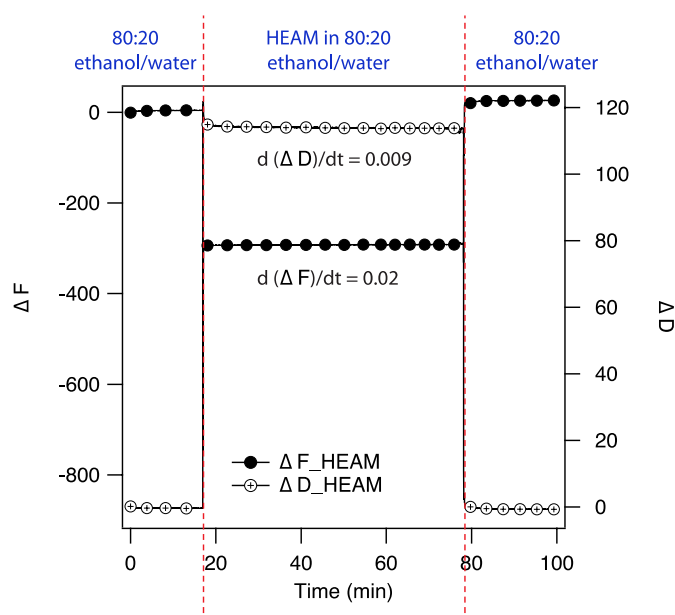


Figure S7. Physisorption of N-hydroxyethylacrylamide (HEAM) on ATRP-initiator modified QCM-sensors, measured by monitoring the variations in the resonance frequency (ΔF) and dissipation (ΔD) as a function of time.

Other than the viscosity induced sharp changes in the ΔF and ΔD upon switching of the medium, the ΔF -t and the ΔD -t profiles remained nearly flat throughout the experiment.

Although this experiment does not account for the solvated monomers trapped inside the tethered polymer chains, it demonstrates that physisorption of monomer on the QCM-D sensor does not influence the ΔF -t and ΔD -t profiles.

References

- [1] M. Davies, Elsevier, **1994**.
- [2] S. Hoffman, D. Briggs, M. Seah, Chichester: Wiley, **1983**.
- [3] M. P. Seah, W. Dench, *Surface and interface analysis* **1979**, *1*, 2-11.
- [4] A. Jablonski, C. Powell, *Journal of electron spectroscopy and related phenomena* **2017**, *218*, 1-12.